International Journal of Mathematical, Engineering and Management Sciences
Vol. 9, No. 2, 205-223, 2024
https://doi.org/10.33889/IJMEMS.2024.9.2.011

Ram Arti Publishers

Advancing Die Design and Optimization through the Combination Approach: A Focus on Spring-back Compensation

Agus Dwi Anggono
Department of Mechanical Engineering,
Universitas Muhammadiyah Surakarta, Jawa Tengah, Indonesia.
Corresponding author: ada126@ums.ac.id

Waluyo Adi Siswanto
Department of Mechanical Engineering,
Universitas Muhammadiyah Surakarta, Jawa Tengah, Indonesia.
E-mail: waluyo@ums.ac.id

Badrul Omar
Department of Manufacturing Engineering,
Universiti Tun Hussein Onn Malaysia, Johor, Malaysia.
E-mail: badrul@uthm.edu.my

Agus Yulianto
Department of Mechanical Engineering,
Universitas Muhammadiyah Surakarta, Jawa Tengah, Indonesia.
E-mail: ay160@ums.ac.id

(Received on September 9, 2023; Revised on November 9, 2023 & January 18, 2024; Accepted on January 26, 2024)

Abstract
This study explores the geometrical deviations that occur in cold stamping, which are caused by the spring-back effects in elastic metals after forming. The primary aim is to introduce and assess the Combination Approach. This approach seamlessly integrates the Displacement Adjustment and Spring Forward methods for die compensation. This multi-stage process meticulously corrects dimensional errors and effectively reduces spring back through iterative processes. Using the NUMISHEET model, numerical simulations have shown a significant reduction in spring back errors, with up to a 55% reduction achieved with optimized die surfaces after five iterations. The proposed Combination Approach improves the accuracy of die design and contributes significantly to the stamping industry by incorporating established techniques within finite element software. This research broadens the scope of die compensation strategies, creating new opportunities for achieving precise die design in stamping.

Keywords- Geometrical deviation, Spring-back, Combination approach, Die compensation, Stamping industries.

1. Introduction

Sheet Metal Forming (SMF) is a widely utilized manufacturing process, particularly in automotive and steel production (Kajal et al., 2023). Despite its proven effectiveness over the years, SMF faces challenges in dealing with the elastic behavior of metal materials, leading to undesirable geometrical deviations known as spring-back. Based on these deviations, spring-back compensation methods have been employed (Darmawan et al., 2019; Lee et al., 2023). However, the current practice of relying on trial and error to determine the optimal surface die design for achieving the desired dimensions has resulted in time-consuming and costly production processes, posing a significant challenge in the stamping industry (Gao et al., 2021; Pangaribawa et al., 2022).

The advent of advanced technologies such as finite element analysis (FEA) and process simulation has significantly enhanced our understanding of the sheet metal forming process. These tools have gained widespread adoption and sophistication within the stamping industries. However, despite their prevalence, FEA software still falls short in accurately predicting spring-back behavior (Atxaga et al., 2022; Lee et al., 2023). This limitation underscores the need to continuously develop and improve numerical solutions in spring-back accommodation. By refining the accuracy of these solutions, we can effectively enhance the overall precision and quality of manufactured products. Such advancements are crucial to meet the ever-increasing demands for higher product accuracy and performance in today's competitive market (Gao et al., 2021).

Spring-back mitigation in cold stamping holds considerable importance and relevance within the industry, primarily due to its consequential influence on the quality and performance of the resulting components. Spring-back refers to the inherent ability of a material to regain its original shape after undergoing deformation. This characteristic can introduce dimensional discrepancies and impact the ultimate form of the stamped component. This phenomenon is particularly significant in aerospace, automotive, and manufacturing, where intricate curved sheet metal components are often employed (Ma and Welo, 2021).

The study conducted by Sun et al. (2022) investigates the compression-spring-back behavior of SUS301 stainless steel gaskets, explicitly focusing on the impact of residual stress. The study introduces a virtual full-cycle testing approach, which integrates gasket stamping, spring back, and compression-spring-back phases using ABAQUS software. The investigation explores the effect of residual stress on compression-spring back performance by utilizing the Hill'48 anisotropic yield model parameters generated by Digital Image Correlation (DIC) for 0.2 mm SUS301 steel. The method's accuracy is validated by comparing it to experimental results. The virtual testing approach systematically investigates the compression-spring-back behaviors of SUS301 stainless steel half-bead gaskets of various sizes. Discussions center around the impact of stamping die geometrical parameters, precisely the width (W) and height (H), as well as the compression load, on the performance of the gasket. The findings highlight the possibility of achieving maximum compression and spring-back rates by modifying the W and H parameters while accommodating different loads. Similar results have been reported in previous investigations undertaken by other researchers (Meng et al., 2022; Xu et al., 2023).

Displacement Adjustment (DA) and Spring Forward (SF) are widely employed strategies for rectifying spring-back through surface modification techniques. Wagoner et al. (2013) introduced the DA method, which involves identifying and manipulating nodes opposite the spring-back region. By deforming the attached blank sheet and comparing its shape with the original, an error is determined and added to the exterior dimensions for compensation. However, a limitation of the DA method is its convergence dependence on the direction of punch movement, making it challenging to shell out the surface region surrounding the dies (Cafuta et al., 2012; Shen et al., 2013). Karafillis and Boyce (1996) proposed the SF technique, compensating for spring-back by multiplying the formed stress state with the residual stress's negative determinant to overcome these limitations. This compensated shape is loaded onto the deformed surface to achieve the desired compensation. The SF method, supported by several researchers, exhibits faster error reduction than other methods (Siswanto and Omar, 2009). Siswanto and Omar introduced an automatic mesh generator for creating new die surfaces after spring forward (Siswanto and Omar, 2009), while Fan et al. (2021) further explored die compensation based on spring forward. Zhang et al. (2013) investigated the compensation direction of the die faces. In general, the SF method offers the advantage of compensating the die surface in various directions, as the deformation is induced by the stresses of the reversed flow in the deformed surface (Lee et al., 2023; Riyadi et al., 2021). However, it is crucial to eliminate specific membrane stresses to prevent unstable solutions resulting from buckling phenomena

during the inversion of stresses. The combination of DA and SF strategies provides a comprehensive approach to spring-back compensation, offering potential solutions for enhancing accuracy and reducing errors in sheet metal forming processes. Continued research and development in this area will further refine and optimize these techniques to meet the increasing demands for precision and quality in the manufacturing industry.

In light of the findings from prior research, it becomes apparent that addressing the issue of die surface compensation requires the seamless integration of both Displacement Adjustment (DA) and Spring Forward (SF) techniques. In responding to this imperative, a novel and inventive solution has been introduced, presenting an alternative technique that adeptly amalgamates DA's and SF's merits. Termed the Combination Approach (CA), this composite compensation technique aims to enhance die-surface accuracy throughout the developmental process. By capitalizing on the advantages offered by both DA and SF techniques, the Combination Approach (CA) augments the outcomes of die compensation. Through the implementation of DA, the initial dimensional errors associated with spring-back are effectively identified and rectified, ensuring a more precise starting point for subsequent phases. Subsequently, the SF method is deployed, leveraging the virtual, inverted internal stress obtained through advanced finite element software. The SF approach refines the compensation process through meticulous die surface adjustments, significantly reducing spring-back faults.

The integration of displacement adjustment (DA) and spring forward (SF) within the Combination Approach (CA) offers a comprehensive and iterative approach to die-compensation, continually refining the dimensions and minimizing spring-back errors. This innovative approach significantly advances the field, enhancing the accuracy and quality of the die surfaces throughout the forming process. By implementing the Combination Approach (CA), manufacturers in industries such as automotive and steel can benefit from improved die design accuracy, reduced production costs, and enhanced overall efficiency. The successful implementation of this method holds the potential to revolutionize die-compensation practices and contribute to the advancement of the stamping industries as a whole.

The study introduces a comprehensive methodology called the Combination Approach (CA) to address die deformations. This approach integrates computational techniques to tackle spring-back issues and enhance the quality of die surfaces. The method significantly augments precision and accuracy in die compensation by employing a series of processes, including node translation using the Displacement Adjustment (DA) algorithm, surface reconstruction, and spring forward (SF) compensation. The primary objective of this systematic approach is to diminish spring-back defects, ultimately improving the quality of stamped items in the stamping sector.

The paper is structured into four distinct sections. The first section provides a comprehensive overview of various methodologies to address the challenges associated with spring-back phenomena in sheet metal forming processes. In particular, the focus is on implementing displacement adjustment and spring forward strategies. The subsequent section presents a detailed description of the study methodology, explicitly outlining the integrated displacement adjustment and spring forward methods. Additionally, it discusses the adopted testing model, the iterative processes undertaken, and the implemented compensation workflow. Section three delves into the effects of spring-back compensation using the proposed combination approach. It examines the impact of compensation variables and iteration counts on the achieved spring-back results. The final two sections of the paper comprise the study's conclusions and a references section that provides a comprehensive list of the cited sources.

2. Research Methodology

Spring-back is commonly defined as the dimensional error in a part that occurs upon the removal of punch load after forming, attributed to the elastic recovery of the material. Thus, the correlation between loading, unloading, and spring-back can be expressed as follows:

$$S_f + S_e + S_p - S_u = 0 \quad (1)$$

$$\left|S_f + S_e - S_d\right| \leq \varepsilon \quad (2)$$

Here, S_f represents the shape formed under total loading, S_e is the shape elastic recovery, and S_u is the unpressed shape. S_p accounts for the non-linear behavior in the unloading shape, which this paper disregards. If the target shape is S_d and the tolerance for shape deviation is ε, the relationship can be expressed as Equation (2). From Equation (2) it is evident that S_f is not identical to S_d because the S_f was modified in the previous approach, and S_e become higher.

The spring forward method introduced a compensation technique that utilizes an opposing internal force after forming, termed the Force Descriptor Method (FDM) (Karafillis and Boyce, 1996). Their approach has demonstrated the capability to reduce spring-back errors by up to 90% after three iterations. The formula for the Force Descriptor Method (FDM) is expressed as follows:

$$S_t^i = g\left(S_d, F_l^{i-1}\right) \quad (3)$$

The function g in this context involves two constant vectors: the desired surface and the internal force F_l^{i-1}. T The fundamental principle of the Force Descriptor Method (FDM) is that following the formation of the final compensated shape S_t^{final}, the part undergoes spring-back toward the desired surface,

$$S_t^{final} = S_d, S_t^{final}.$$

The Combination Approach (CA) integrates Displacement Adjustment (DA) and Spring Forward (SF) methodologies for efficient die compensation. A detailed examination of its operational principles and procedures is presented below. Figure 1 illustrates the application of CA in the die compensation process.

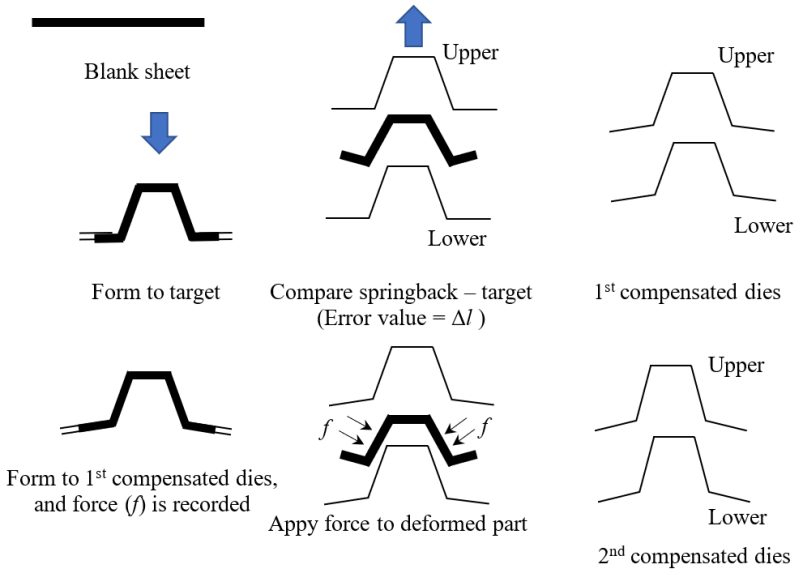

Figure 1. Combination approach to compensate spring-back.

To initiate the compensation process, CA utilizes a model blank surface, which is deformed to match either the original die surface or the desired target die surface. This research used the widely acclaimed Auto form software to form the simulation and provide the necessary reference geometry and spring-back data for analysis. The original node data is extracted from the deformed blank surface, capturing its initial shape after forming. After the punch is removed, the distorted shape springs back, establishing new data points for the positions of the spring-back nodes.

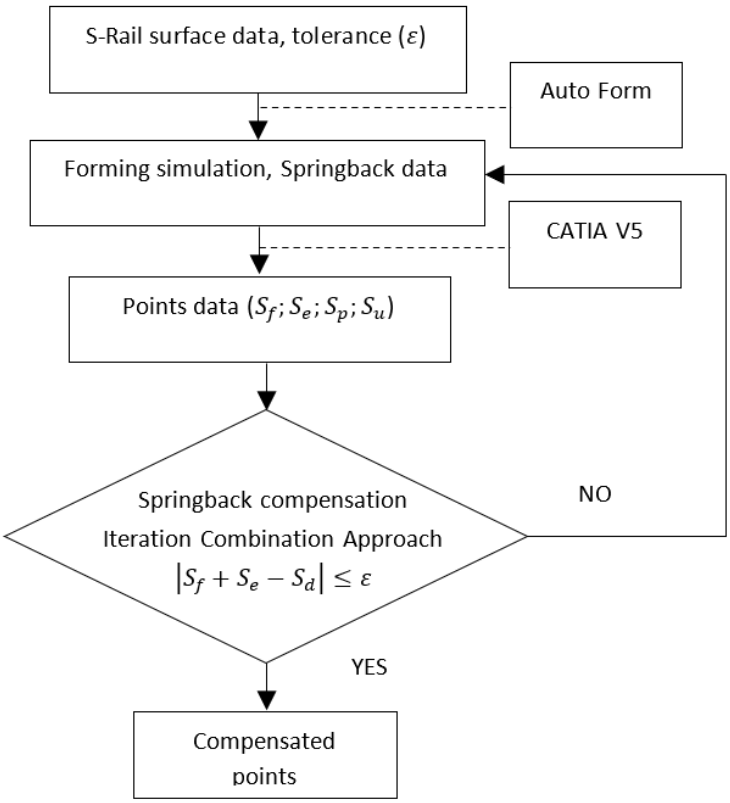

Figure 2. The process of spring-back compensation through the implementation of the combination approach.

The compensation procedure adheres to a meticulously constructed flowchart, as depicted in Figure 2. The above-provided flowchart outlines the sequential steps involved in the Combination Approach (CA) technique, visually representing the compensation process and its primary stages. Applying the Combination Approach in die compensation illustrates a comprehensive methodology that integrates various computational and analytical techniques. The CA system offers an efficient method for addressing spring-back defects and enhancing the optimization of die surfaces. This objective is achieved through deploying advanced software, meticulous initial and spring-back node data collection, and strict adherence to a systematic flowchart methodology.

Integrating Displacement Adjustment (DA) and Spring Forward (SF) approaches within the CA methodology presents a promising avenue for improving the precision and accuracy of die compensation. The method illustrated in Figure 2 enhances the compensation procedure, thereby facilitating improved regulation of the die surfaces. Consequently, this optimization contributes to higher efficiency and quality within the stamping industries.

The subsequent Combination Approach (CA) phase involves translating nodes to accommodate the die form effectively. This is accomplished by utilizing the algorithm derived from the Displacement Adjustment technique. The translation technique relies on the spring-back results obtained from the prior analysis, which determine the required adjustment distance for the nodes. The outcome of this particular stage yields a mesh surface that serves as the adjusted die shape.

The CA ensures the alignment of the produced die surface with the intended dimensions and the effective minimization of spring-back faults through precise calculation and implementation of the required node translations. The critical translation step is pivotal in achieving optimal precision and accuracy in the compensation process. Ultimately, it enhances the overall quality and performance of the stamped products.

The reference geometry $\vec{R}$ is defined as a compilation of n points in $\Re^3$. $\vec{S}$ represents the surface geometry after spring-back. Figure 3 illustrates the translation of nodes from their original positions to the compensated positions.

$$\vec{R} = \{\vec{r_i} | \vec{r_i} \in \Re^3, 1 \leq i \leq n\} \quad (4)$$

$$\vec{S} = \{\vec{S_i} | \vec{S_i} \in \Re^3, 1 \leq i \leq n\} \quad (5)$$

$$\vec{C} = \vec{R} + a(\vec{S} - \vec{R}) \; ; \vec{c_i} = \vec{r_i} + a(\vec{s_i} - \vec{r_i}) \quad (6)$$

$$C_x = R_x + (S_x - R_x) \quad (7)$$

$$C_y = R_y + (S_y - R_y) \quad (8)$$

$$C_z = R_z + (S_z - R_z) \quad (9)$$

To determine the compensated surface geometry $\vec{C}$, the reference and spring-back nodes with a similar number i when coupled, $\vec{r_i}$ turns to $\vec{s_i}$ after being unloaded. The factor a referred to as the compensation factor. In the Displacement Adjustment (DA) concept, it is generally assumed to be a factor of 1.0, signifying the complete translation of the vector. The objective of the translation is to find the compensation in all directions (x, y, z), as defined in Equations (7-9).

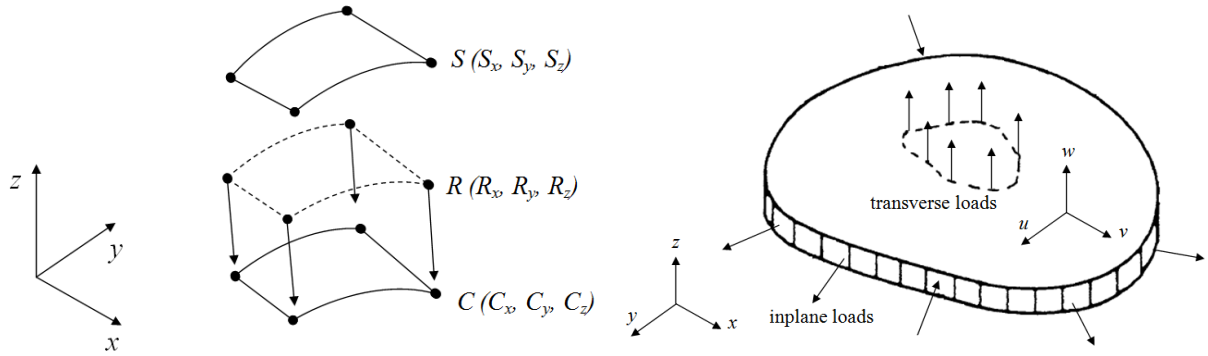

Figure 3. Node translation for compensation, inplane, and transverse loads.

The third step involves surface reconstruction. The compensated nodes of the die are then transformed into the surface model using CATIA software. The essential surface data of punch, die, and blank holder are reconstructed in this phase. The newly designed punch and blank holder surface are called the compensated die surface, representing the blank thickness. A new forming simulation is subsequently conducted using the freshly compensated dies. After spring-back, the error, under its tolerance, is determined by comparing

the shape with its target. The output of residual stresses is generated in this step, which will be utilized in the next compensation iteration.

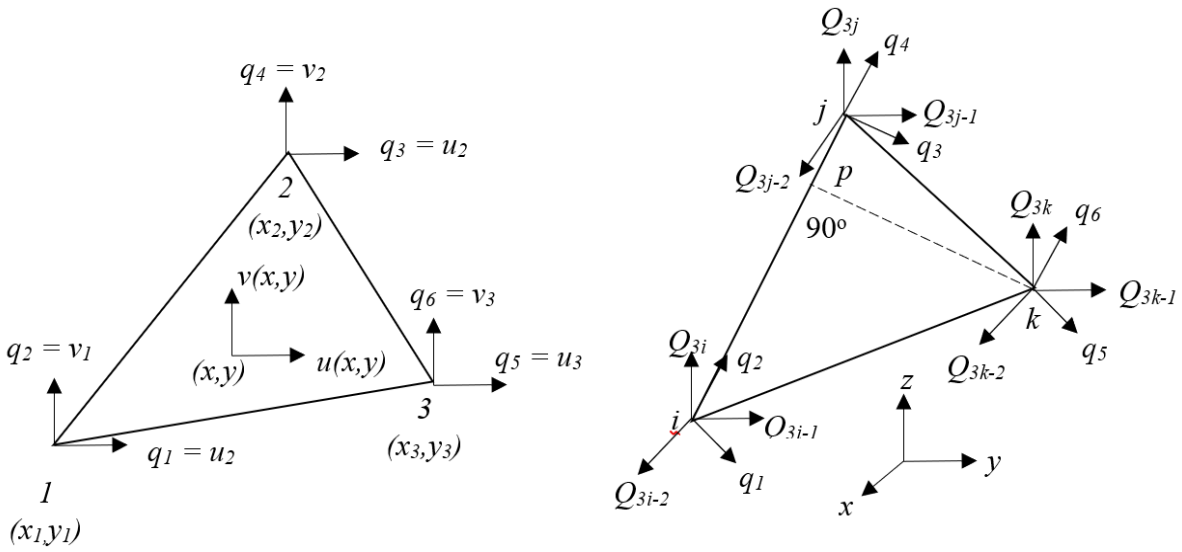

Figure 4. Triangular element, global and local coordinates.

The fourth step involves compensating the dies using the Spring Forward (SF) algorithm. The application of residual stress to the deformed shape in this step poses a complex engineering problem. Therefore, the finite element method is employed to determine a precise solution. A flat surface exposes both in-plane and transverse loads, as depicted in Figure 3. Points representing the metal plate can experience displacement denoted as *u*, *v*, and *w*, parallel to the *x*, *y*, and *z*-axes. The triangular element is examined in analyzing the thin plate, as illustrated in Figure 4. The displacement variation of *u* and *v* across the thickness can be formulated in terms of *w*, as,

$$u = -z\frac{\partial w}{\partial x}; \quad and \quad v = -z\frac{\partial w}{\partial y} \tag{10}$$

$$\varepsilon_x = \frac{\partial u}{\partial x} = -z\frac{\partial^2 w}{\partial x^2} = \kappa_x z \tag{11}$$

$$\varepsilon_y = \frac{\partial u}{\partial y} = -z\frac{\partial^2 w}{\partial y^2} = \kappa_y z \tag{12}$$

$$\gamma_{xy} = \frac{\partial u}{\partial y} + \frac{\partial v}{\partial x} = -2\kappa_{xy} z \tag{13}$$

$$\kappa_x = -\frac{\partial^2 w}{\partial x^2}, \quad \kappa_y = -\frac{\partial^2 w}{\partial y^2}, \quad \kappa_{xy} = -2\frac{\partial^2 w}{\partial x \partial y} \tag{14}$$

For thin plates, $\gamma_{xy} = \gamma_{yz} = 0$. The stress-strain relation for isotropic material is given by,

$$\begin{Bmatrix} \sigma_x \\ \sigma_y \\ \tau_{xy} \end{Bmatrix} = \frac{Ez}{1-v^2} \begin{bmatrix} 1 & v & 0 \\ v & 1 & 0 \\ 0 & 0 & \frac{1-v}{2} \end{bmatrix} \begin{Bmatrix} \kappa_x \\ \kappa_y \\ \kappa_{xy} \end{Bmatrix} \tag{15}$$

The moments M_x, M_y, and M_{xy} are given by,

$$\begin{Bmatrix} M_x \\ M_y \\ M_{xy} \end{Bmatrix} = D \begin{bmatrix} 1 & v & 0 \\ v & 1 & 0 \\ 0 & 0 & \frac{1-v}{2} \end{bmatrix} \begin{Bmatrix} \kappa_x \\ \kappa_y \\ \kappa_{xy} \end{Bmatrix} \quad (16)$$

where, the flexural rigidity $D = EI = \frac{Eh^3}{12(1-v^2)}$.

To facilitate the matrix transformation $[\lambda]$, it is essential to establish the directional parameters of lines *ox* and *oy*, including their respective cosines concerning the X, Y, and Z axes. Focusing on line *oy*, its direction cosines resemble those of line *ij*. Consequently, we derive the following expressions:

$$l_{ij} = \frac{X_j - X_i}{d_{ij}} \quad (17)$$

$$m_{ij} = \frac{Y_j - Y_i}{d_{ij}} \quad (18)$$

$$n_{ij} = \frac{Z_j - Z_i}{d_{ij}} \quad (19)$$

Here, the subscripts *i* and *j*, along with d_{ij} denote the points under consideration and the magnitude of the vector between them, respectively, calculated as:

$$|d_{ij}| = \left[(X_j - X_i)^2 + (Y_j - Y_i)^2 + (Z_j - Z_i)^2 \right]^{1/2} \quad (20)$$

The alignment of line *ox* with the cosine direction coincides with that of line *pk*.

$$l_{pk} = \frac{X_k - X_p}{d_{pk}} \quad (21)$$

$$m_{pk} = \frac{Y_k - Y_p}{d_{pk}} \quad (22)$$

$$n_{pk} = \frac{Z_k - Z_p}{d_{pk}} \quad (23)$$

The variable d_{pk} represents the distance between points *p* and *k*. Consequently, the computation of coordinates (X_p, Y_p, Z_p) for point p within the global coordinate system can be deduced as follows:

$$X_p = X_i + l_{ij}\, d_{ip} \quad (24)$$

$$Y_p = Y_i + m_{ij}\, d_{ip} \quad (25)$$

$$Z_p = Z_i + n_{ij}\, d_{ip} \quad (26)$$

The variable d_{ip} signifies the distance or gap between points, specifically points *p* and *i*. Determining the d_{ip} value involves applying the condition that lines *ij* and *pk* are mutually perpendicular.

The stresses contribute to the load vector.

$$\overrightarrow{P_s^{(e)}} = \iint_{S_1^{(e)}} [N]^T \begin{Bmatrix} P_{xo} \\ P_{yo} \end{Bmatrix} dS_1 \quad (27)$$

The variables P_{xo} and P_{yo} are treated as constant values in this context. The $\overrightarrow{P_s^{(e)}}$ vector comprises three distinct components corresponding to different sides of the element. When the surfaces connecting nodes 1 and 2 experience surface stresses with magnitudes P_{xo} and P_{yo}, the resulting outcome is determined as follows:

$$\overrightarrow{P_s^{(e)}} = \iint_{S_1^{(e)}} \begin{bmatrix} N_1 & 0 \\ 0 & N_1 \\ N_2 & 0 \\ 0 & N_2 \\ N_3 & 0 \\ 0 & N_3 \end{bmatrix} \begin{Bmatrix} P_{xo} \\ P_{yo} \end{Bmatrix} dS_1 = \frac{S_{12}}{2} \begin{Bmatrix} P_{xo} \\ P_{yo} \\ P_{xo} \\ P_{yo} \\ 0 \\ 0 \end{Bmatrix} \quad (28)$$

The variable S_{12} represents the surface area encompassing nodes 1 and 2.

The residual stress-induced deflection of the shape was effectively compensated for during the forming simulation. Nodes were generated based on this position, and the die surface was constructed accordingly. The forming simulation utilized the newly compensated die surface, and spring-back was assessed for tolerance. If the deviation exceeded the acceptable range, iterative adjustments were implemented until the error fell within the specified tolerance.

A die surface generated using the Combination Approach was applied in the Autoform software to evaluate the precision of the established hybrid algorithm for die compensation. This process entailed simulating spring-back and comparing it with the reference surface. The hybrid die shape was integrated into Autoform, and finite elements were modified to complete the binder and punch parts. They facilitated the modeling of a die surface for spring-back calculation in Autoform, with the results from the Combination Approach being compared to those obtained from the Autoform spring-back prediction.

This study conducted simulations involving the die, binder, punch, and reference surface. The input data was used to determine the deviation distance error by comparing the results with the reference geometry. When the deviation exceeded a significant threshold, software utilizing the DA algorithm was employed. Further simulations were conducted with an adjusted die surface until the deviation was within the tolerance limit.

This research compared the results obtained from the CA technique with those derived from the DA and SF methodologies. The evaluation included determining the maximum error, the number of iterations in each cycle, and the total CPU time required to achieve convergence of the compensated die surfaces.

The displacement model adheres to the standard constant strain triangle (CST) finite element formulation, imposing a linear displacement within the element. The displacement is represented as follows:

$$u(x,y) = \alpha_1 + \alpha_2 x + \alpha_3 y \quad (29)$$

$$v(x,y) = \alpha_4 + \alpha_5 x + \alpha_6 y \quad (30)$$

the constants α_1 through α_6 are defined with the nodal degrees of freedom, resulting in the following displacement model:

$$\vec{U} = \begin{Bmatrix} u(x,y) \\ v(x,y) \end{Bmatrix} = [N]\overrightarrow{q^{(e)}} \quad (31)$$

where,

$$[N(x,y)] = \begin{bmatrix} N_1(x,y) & 0 & N_2(x,y) & 0 & N_3(x,y) & 0 \\ 0 & N_1(x,y) & 0 & N_2(x,y) & 0 & N_3(x,y) \end{bmatrix} \quad (32)$$

$$N_1(x,y) = \frac{1}{2A}[y_{32}(x - x_2) - x_{32}(y - y_2)] \quad (33)$$

$$N_2(x,y) = \frac{1}{2A}[y_{31}(x - x_3) - x_{31}(y - y_3)] \quad (34)$$

$$N_3(x,y) = \frac{1}{2A}[y_{21}(x - x_2) - x_{21}(y - y_1)] \quad (35)$$

A is the surface area of the triangle,

$$A = \frac{1}{2}(x_{32}y_{21} - x_{21}y_{32}) \quad (36)$$

The strain associated with the two-dimensional element is given by,

$$\vec{\varepsilon} = \begin{Bmatrix} \varepsilon_{xx} \\ \varepsilon_{yy} \\ \varepsilon_{xy} \end{Bmatrix} = \begin{Bmatrix} \frac{\partial u}{\partial x} \\ \frac{\partial v}{\partial y} \\ \frac{\partial u}{\partial x} + \frac{\partial v}{\partial y} \end{Bmatrix} \quad (37)$$

The components of strain can be expressed in nodal displacements as follows,

$$\vec{\varepsilon} = [B]\,\overrightarrow{q^{(e)}} \quad (38)$$

where,

$$[B] = \frac{1}{2A}\begin{bmatrix} y_{32} & 0 & -y_{31} & 0 & y_{21} & 0 \\ 0 & -x_{32} & 0 & x_{31} & 0 & -x_{21} \\ -x_{32} & y_{32} & x_{31} & -y_{31} & -x_{21} & y_{21} \end{bmatrix}. \quad (39)$$

The relations of stress-strain given by,

$$\vec{\sigma} = [D]\,\vec{\varepsilon} \quad (40)$$

The stiffness matrix of the element $\left[k^{(e)}\right]$ can be obtained by,

$$\left[k^{(e)}\right] = \iiint_{V^{(e)}} [B]^T [D][B]\, dV \quad (41)$$

where, $V^{(e)}$ denotes the volume of the element.

Consider nodes 1, 2, and 3, corresponding to elements associated with nodes *i*, *j*, and *k* in the global system. A local coordinate system, denoted as *xy*, is established with its origin at node 1, also known as node i. As depicted in Figure 4, the *y*-axis is aligned along the edges connecting nodes 1 and 2 (edge *ij*). At the same time, the *x*-axis is oriented perpendicularly to the *y*-axis and directed towards node 3 (node *k*).

The numerical simulation of spring-back compensation is demonstrated using Autoform software. The 3D (three-dimensional) spring-back model was derived from the NUMISHEET2008 S-rail design, which serves as the benchmark model, along with an additional spring-back-related problem. The finite element simulation was conducted using Autoform to analyze the behavior of the rigid tooling in deep drawing, which includes a die, blankholder, punch, and distance plate, as shown in Figure 5.

The spring-back compensation method involved a meticulous numerical analysis, employing the Autoform program to facilitate the extraction and simulation of a 3D spring-back model. The chosen benchmark model from NUMISHEET2008 served as a reference for comparison, while an additional problem was introduced to enable a comprehensive evaluation of spring-back characteristics. The use of Autoform allowed for a thorough analysis of the inflexible tooling elements, namely the die, blankholder, punch, and

distance plate, providing valuable insights into the spring-back phenomenon in the deep drawing process.

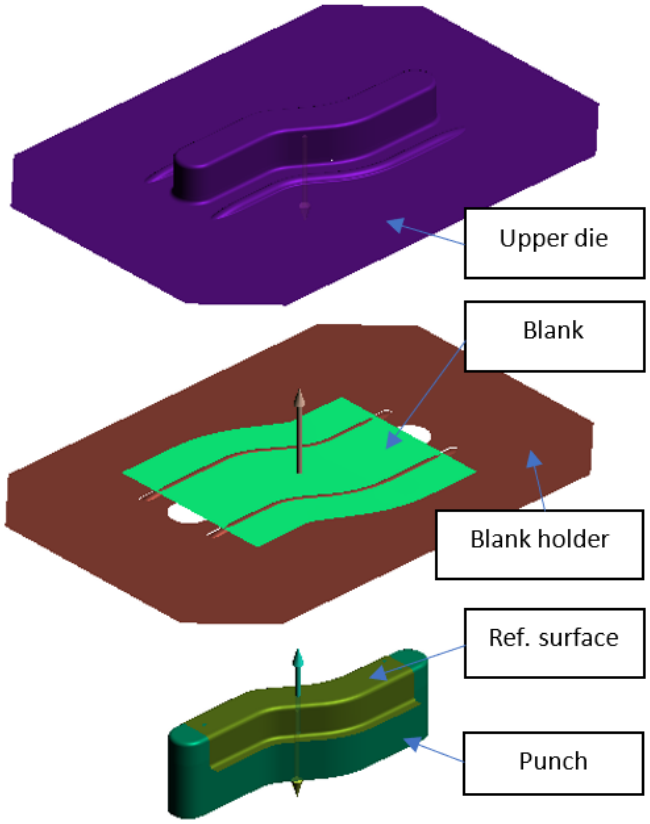

Figure 5. Assembly of S-Rail model.

The assessment of spring-back outcomes necessitates a comprehensive examination of various sources, systematically classified into Sections A, B, C, and D, as depicted in Figure 6. HX260LAD steel was thoughtfully selected from the material library for the cold-forming simulation due to its suitability for the intended application. To effectively evaluate the spring-back characteristics and their impact on the produced component, a thorough understanding of the mechanical properties of the blank material was imperative. This essential data is conveniently summarized in Table 1, providing a comprehensive overview of the material's characteristics, including its yield strength, ultimate tensile strength, and elastic modulus, among other pertinent properties.

Table 1. The mechanical characteristics of HX260LAD.

Orient	Thick mm	Yield Stress MPa	U.T.S MPa	Uniform Elong. %	r-Value
L	1.0	394.3	463.7	16.4	0.581
T	1.0	427.7	466.0	17.5	1.013
D	1.0	395.3	447.0	17.0	1.166
Mean	1.0	405.8	458.9	16.9	0.981

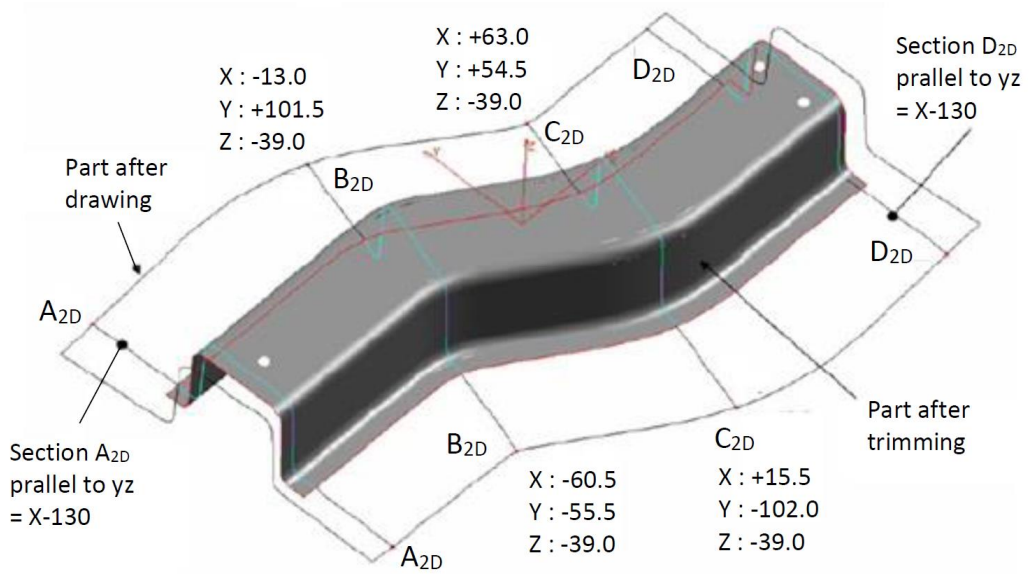

Figure 6. Spring-back observation sectioning and clamps positioning.

3. Results and Discussion

This study aims to investigate the analysis of spring-back and the various compensation methods used in sheet metal forming processes. The spring-back analysis was carried out with a specified blank holder force (BHF) of 150 kN, using a frictionless smooth-bead binder. The study revealed a significant spring-back deviation, with measurements as high as 1.87 mm observed in the initial die surface design. Based on these preliminary spring-back results, a compensation procedure was developed using the direct compensation approach. Several researchers have applied these compensation processes to increase the rigor and robustness of the investigation (Meng et al., 2022; Xu et al., 2023). The insights gained from this study contribute significantly to sheet metal forming, providing valuable perspectives on effective strategies for reducing spring-back and improving the formability process.

Initially, the compensating efforts faced challenges due to Autoform's limitations in adequately considering the binder's shape planar nature. It resulted in difficulties achieving a smooth and continuous connection between the binder and die surface, leading to an unsatisfactory experimental attempt. Tight adherence of the binder to the die surface during compensation is crucial for effective mitigation. To address this challenge, engineers proactively redesigned the binder with a perpendicular surface construction on its flat section to optimize its integration with the die surface. This modification significantly enhanced the accuracy and dependability of the compensation procedure, enabling the binder to adhere tightly to the die surface and minimize spring-back deviations.

The effectiveness of the binder modification was comprehensively assessed in subsequent trials through rigorous testing. The revised geometry successfully addressed the initial constraints, resulting in improved precision in forming and a reduction in spring-back deviation. This pivotal alteration has significant implications for enhancing the compensation process, providing valuable insights for advancing sheet metal forming procedures, and contributing to continuous improvement in the sector, as Gang wants et al. (2022) addressed.

The compensation phase that followed extended beyond the surface of the die to encompass the surfaces of

the punch and binder as well. It was done to ensure uniformity and consistency in the gap throughout the entire forming process. The research team conducted an in-depth examination of compensation factors, considering values ranging from 0.05 to 2.0, with the aim of achieving the most favorable outcomes. The primary objective of this study was to determine the compensation factor that resulted in the lowest spring-back value. This finding would then serve as a foundation for improving future compensation cycles.

The researchers conducted a series of systematic experiments to assess the impact of various compensation factors on spring-back reduction. They aimed to achieve a balanced and optimal compensation strategy by considering the effects on different surfaces, such as the die, punch, and binder. The comprehensive examination of the factors resulted in a more accurate and effective compensation procedure, which improved the forming accuracy and reduced the spring-back problems. The outcomes of this inquiry provided valuable insights for future iterations and laid the foundation for advancing spring-back compensation techniques in sheet metal forming applications.

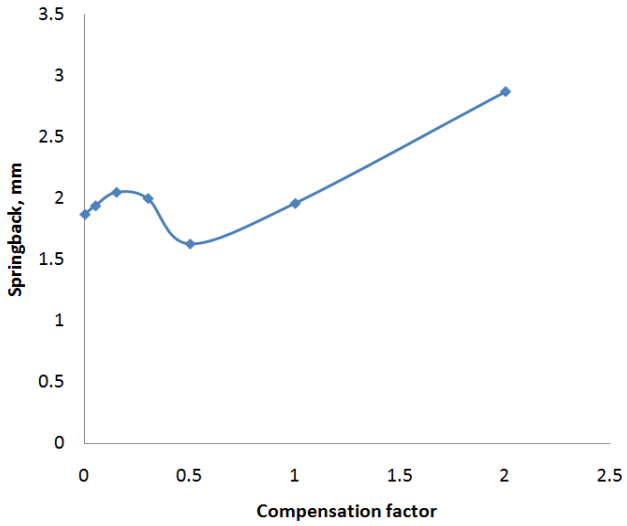

Figure 7. Spring-back results in a variation of compensation factors.

The graph shows the relationship between different compensation components and their corresponding spring-back outcomes, as shown in Figure 7. The graphic was obtained by calculating the average spring-back values in sections A, B, C, and D of the S-rail model, as illustrated in Figure 6, consistent with the referenced work (Zhang et al., 2016). The x-axis represents a range of compensation factors from 0 to 2.5. The y-axis shows the spring-back outcomes, measured in millimeters (mm). As the compensation factor increases, a noticeable trend emerges in the spring-back outcomes. The spring-back values increase slightly from 1.8 mm to 2.2 mm for compensation factors of 0.05 and 0.15, followed by a slight decrease to 2.1 mm for the compensation factor of 0.3. It indicates that applying the compensation factor increases the spring-back tendency, which suggests the possibility of overcorrection during the forming process.

However, with the increase in the compensation factor to 0.5, a substantial improvement in the spring-back outcome is observed, resulting in a reduction of 1.6 mm. It implies adopting a more efficient compensation strategy for minimizing spring-back, leading to better alignment between the formed portion and the die surface. Notably, when the compensation factor is set to 2, there is a noticeable increase in spring-back to a magnitude of 2 mm. This observation suggests the existence of a potential threshold where excessive compensation may be occurring. The graph demonstrates a significant rise in spring-back, reaching 3 mm

when the compensation factor exceeds 2.5. It indicates that an excessive level of compensation has led to a deviation from the intended formed shape.

In summary, the graph illustrates that a compensation factor of 0.5 yields the most favorable spring-back value of 1.6 mm, indicating an optimal balance between compensation and precision in the forming process. This information is of considerable importance as it assists in determining the appropriate compensation factor to achieve the necessary dimensional accuracy in sheet metal forming procedures. The graph illustrates the correlation between the number of iterations and their respective spring-back results, as presented in Figure 8 for each section and the mean results. The x-axis represents the iteration number, ranging from 0 to 5, while the y-axis indicates the spring-back results, measured in millimeters (mm). The compensation factor employed for these iterations was 0.5.

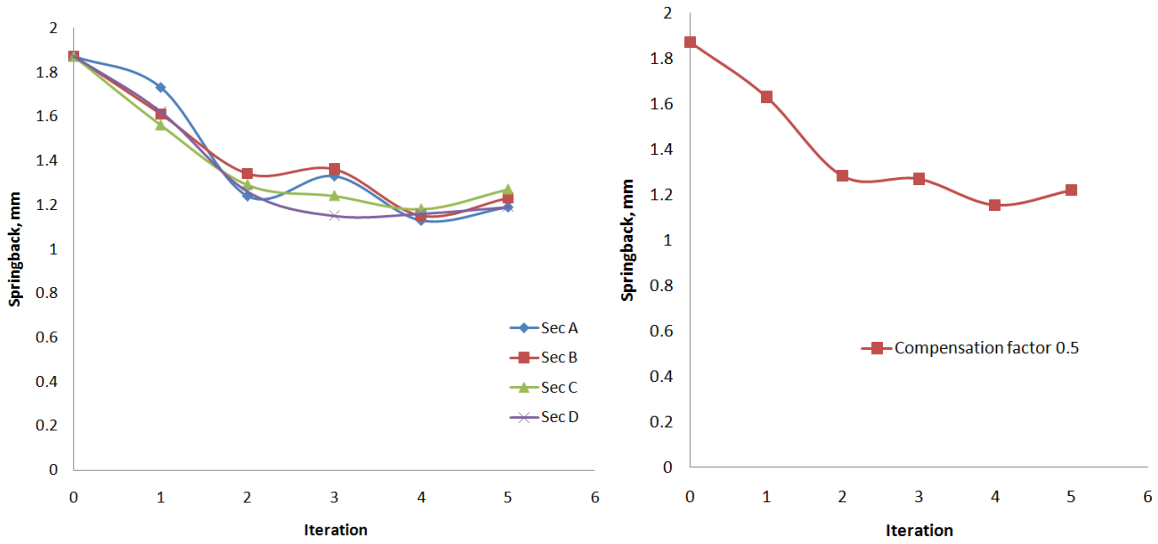

Figure 8. The spring-back outcomes observed in each iteration of S-rail compensation for sections A, B, C, and D, as well as the average spring-back value for each iteration.

The graph reveals a clear trend of decreasing spring-back values as the number of iterations increases. With no compensation applied, the initial spring-back value is 1.92 mm (iteration number = 0). This value drops significantly to 1.76 mm after one iteration of the compensation process. The compensation process has effectively corrected the initial spring-back deviation, improving forming accuracy. This finding aligns with other studies (Fan et al., 2021; Gang wants et al., 2022).

The iterative approach used in this study demonstrates its effectiveness in reducing spring-back and enhancing the dimensional accuracy of the formed component. The spring-back value decreases from 1.87 mm in the initial state to 1.34 mm in the second iteration, indicating a significant improvement in the compensation process. The trend continues in the subsequent iterations, with the spring-back value reaching 1.26 mm in the third iteration and 1.15 mm in the fourth iteration. These results suggest that the compensation process is converging towards the optimal forming condition, as each iteration reduces the spring-back error and increases the accuracy of the component. In the fifth and final iteration, the spring-back value is 1.22 mm, slightly higher than the previous iteration but still lower than the initial state. It implies that the compensation process has reached a stable and refined state, with marginal changes in the

spring-back value. The overall spring-back reduction achieved by this method is 38.5%, which is superior to the results reported by other researchers (Hetz et al., 2020; Hou et al., 2021).

In summary, the graph illustrates the impact of increasing iterations on spring-back behavior, with each iteration contributing to improved forming accuracy and reduced spring-back deviation. The iterative compensation approach effectively enhances the dimensional precision of the formed part and optimizes the sheet metal forming process.

The comparison between the Combination Approach (CA) and Autoform in reducing spring-back is depicted through two separate graphs, each illustrating the spring-back results at different iteration numbers, as shown in Figure 9. The x-axis represents the iteration number, ranging from 0 to 5, while the y-axis indicates the spring-back results, measured in millimeters (mm).

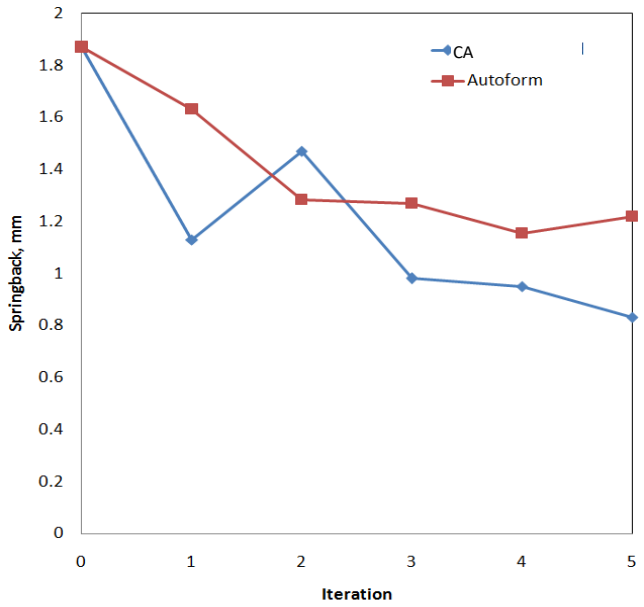

Figure 9. The spring-back outcomes of the CA and Autoform software packages were examined.

For the Combination Approach, the graph demonstrates a clear trend in the spring-back values as the number of iterations increases. At the initial stage, with 0 iterations (iteration number = 0), the spring-back result is recorded as 1.92 mm. As the number of iterations progresses to 1, there is a substantial reduction in spring-back to 1.16 mm, indicating the immediate effectiveness of the CA in minimizing spring-back deviation. In the second iteration, a slight increase in the spring-back value to 1.53 mm is observed, suggesting the need for additional refinement. Nevertheless, the CA shows noteworthy advancements in its third iteration, with a reduction in spring-back to 1.16 mm. This outcome highlights the CA's capacity to approach ideal precision in forming.

The fourth iteration of the experiment continues the observed trend with a spring-back value of 0.98 mm. This result signifies a consistent and significant reduction in spring-back deviation. After five iterations, the spring-back result reaches a noteworthy magnitude of 0.83 mm, demonstrating the commendable precision achieved by the Combination Approach (CA) system in mitigating spring-back and enhancing the dimensional precision of the manufactured component.

In contrast, the Autoform graph illustrates a comparable pattern in spring-back reduction as the number of iterations increases. Starting with an initial iteration of 0. the spring-back outcome is observed to be 1.92 mm, closely aligning with the initial spring-back value of the CA. In the initial iteration, the Autoform approach demonstrates a spring-back value of 1.76 mm, indicating its ability to mitigate the initial spring-back deviation effectively. Autoform consistently improves the compensation process as the iterations progress, leading to a gradual decrease in spring-back values. Specifically, for iteration numbers 2, 3, and 4, the spring-back values are observed to be 1.34 mm, 1.26 mm, and 1.15 mm, respectively. After undergoing five iterations, the spring-back measurement reaches a value of 1.22 mm. This finding supports the effectiveness of the Autoform approach in consistently improving the precision of forming processes and reducing spring-back deviation, as noted by other researchers (Yaguang et al., 2019; Meng et al., 2022; Gang wants et al., 2022).

In summary, the comparison between the Combination Approach and Autoform reveals that both methods effectively decrease spring-back deviation as the number of iterations increases. While the Combination Approach demonstrates slightly superior performance, both techniques showcase significant improvements in dimensional accuracy through iterative compensation. The findings provide valuable insights into the capabilities of these methods in optimizing sheet metal forming processes and reducing spring-back-induced challenges. The decrease in spring-back errors discovered carries significant implications for real manufacturing scenarios, including improved product quality, cost savings, enhanced efficiency, minimized rejections and rework, and increased reliability (Choi et al., 2020).

Minimizing spring-back faults ensures that stamped components conform to the desired design specifications. Improved precision produces high-quality goods that meet the specified dimensional tolerances and structural requirements, enhancing product quality (Wei et al., 2019). Mitigating spring-back errors has the potential to reduce material waste and subsequently lower production costs. When components effectively retain their desired shape after manufacturing, the need for corrective actions or additional procedures is minimized, leading to optimized resource utilization (Elghawail et al., 2017).

Reducing spring-back faults enhances the efficiency of manufacturing processes. Spring-back reduction facilitates seamless production flows and potentially increases overall throughput by minimizing the time and effort spent on adjusting and rectifying inaccuracies (Gomes et al., 2017). A decrease in spring-back faults leads to fewer rejected components due to dimensional discrepancies. This reduction in rejected products and rework minimizes production downtime and associated costs, further enhancing overall process efficiency (Suckow et al., 2021).

Products with reduced spring-back errors generally exhibit enhanced reliability and consistency in their performance. Reliability is paramount in industries prioritizing accuracy and consistency, such as aerospace or automotive manufacturing (Zhu et al., 2013). Enhanced understanding and mastery of spring-back errors empower engineers to expand the scope of design possibilities. Manufacturers gain confidence in exploring complex shapes and geometries, knowing that the employed compensation techniques can adequately address spring-back concerns (Ma and Welo, 2021).

4. Conclusion

The study gap lacks a comprehensive investigation or a well-established methodology that effectively integrates and optimizes the benefits of Displacement Adjustment (DA) and Spring Forward (SF) procedures within a unified and novel framework. This gap underscores the need for further research and refinement of a methodology that combines both approaches to achieve enhanced precision and efficiency in compensating for die surface irregularities. It effectively addresses the challenges posed by the spring-

back phenomena encountered in sheet metal forming processes. The Combination Approach (CA), which amalgamates DA and SF, has yielded robust and accurate results in compensating for spring-back.

This study successfully demonstrated die surface creation from point clouds using CATIA V5. However, it is noteworthy that the processed and results data, stored in text format, can lead to large file sizes, significantly depending on the model's complexity. For future applications, considering a conversion to binary format could potentially improve the iteration process and reduce file size. Additionally, ongoing efforts aim to extend the algorithm further to automate mesh or surface generation without requiring CAD software involvement. The Combination Approach algorithm has demonstrated great promise as an alternative spring-back compensation technique, achieving a remarkable 55% reduction after five iteration cycles, surpassing another comparison method which only achieved a 33% reduction. This exceptional performance highlights its potential for enhancing the accuracy of metal product stamping processes.

The successful validation of the CA algorithm in an S-rail model, with inputs and outputs of node coordinates, further enhances its user-friendliness and practicality for convenient implementation. The significance of this research lies in the CA algorithm's capability to serve as one of the approaches used to accommodate spring-back and improve the accuracy of stamped products, especially when working with highly elastic materials. With the potential applicability in the die stamping industries, the CA algorithm presents a valuable contribution to the field and holds promise for enhanced manufacturing processes. The next objective is to investigate the potential of the CA algorithm in minimizing spring-back in different materials and adapting it to address various production difficulties.

Conflict of Interest

The authors declare that there are no conflicts of interest to declare with this publication.

Acknowledgments

The authors gratefully acknowledge the generous financial assistance and unwavering support provided by the Innovation and Research Centre and Faculty of Engineering at Universitas Muhammadiyah Surakarta throughout this research project. The project was funded by grants under contract numbers 145.5/A.3-III/LRI/VII/2022 and 231/A.3-III/FT/VI/2022.

References

Atxaga, G., Arroyo, A., & Canflanca, B. (2022). Hot stamping of aerospace aluminium alloys: Automotive technologies for the aeronautics industry. *Journal of Manufacturing Processes*, *81*, 817-827. https://doi.org/10.1016/j.jmapro.2022.07.032.

Cafuta, G., Mole, N., & Štok, B. (2012). An enhanced displacement adjustment method: Spring-back and thinning compensation. *Materials and Design*, *40*, 476-487. https://doi.org/10.1016/j.matdes.2012.04.018.

Choi, Y., Lee, J., Panicker, S.S., Jin, H.K., Panda, S.K., & Lee, M.G. (2020). Mechanical properties, spring-back, and formability of W-temper and peak aged 7075 aluminum alloy sheets: Experiments and modeling. *International Journal of Mechanical Sciences*, *170*, 105344. https://doi.org/10.1016/j.ijmecsci.2019.105344.

Darmawan, A.S., Anggono, A.D., & Nugroho, S. (2019). Spring-back phenomenon analysis of tailor welded blank of mild steel in U-bending process. *AIP Conference Proceedings*, *2114*(1), 030021. https://doi.org/10.1063/1.5112425.

Elghawail, A., Essa, K., Abosaf, M., Tolipov, A., Su, S., & Pham, D. (2017). Prediction of spring-back in multi-point forming. *Cogent Engineering*, *4*(1), 1400507. https://doi.org/10.1080/23311916.2017.1400507.

Fan, Y., Liu, C., & Wang, J. (2021). Prediction algorithm for spring-back of frame-rib parts in rubber forming process by incorporating Sobol within improved grey relation analysis. *Journal of Materials Research and Technology*, *13*, 1955-1966. https://doi.org/10.1016/j.jmrt.2021.05.102.

Gang wants, Z., Qinghua, W., Ranyang, Z., Zhenghua, G., Maozi, T., & Xianwen, Y. (2022). Simulation analysis of spring-back of ultra-thin-walled corrugated ring rubber forming. *Journal of Plastic Engineering*, *29*(5), 39-44. https://doi.org/10.3969/j.issn.1007-2012.2022.05.005.

Gao, M., Wang, Q., Li, L., Xiong, W., Liu, C., & Liu, Z. (2021). Emergy-based method for evaluating and reducing the environmental impact of stamping systems. *Journal of Cleaner Production*, *311*, 127850. https://doi.org/10.1016/j.jclepro.2021.127850.

Gomes, T., Silva, F.J.G., & Campilho, R.D.G.S. (2017). Reducing the simulation cost on dual-phase steel stamping process. *Procedia Manufacturing*, *11*, 474-481. https://doi.org/10.1016/j.promfg.2017.07.138.

Hetz, P., Suttner, S., & Merklein, M. (2020). Investigation of the Spring-back behaviour of high-strength aluminium alloys based on cross profile deep drawing tests. *Procedia Manufacturing*, *47*, 1223-1229. https://doi.org/10.1016/j.promfg.2020.04.187.

Hou, H., Zhao, G., Chen, L., & Li, H. (2021). Anisotropic spring-back models of FCC metal material under severe plastic compressive deformation. *International Journal of Mechanical Sciences*, *202-203*, 106513. https://doi.org/10.1016/j.ijmecsci.2021.106513.

Kajal, G., Tyagi, M.R., & Kumar, G. (2023). A review on the effect of residual stresses in incremental sheet metal forming used in automotive and medical sectors. *Materials Today: Proceedings*, *78*(part 3), 524-534. https://doi.org/10.1016/j.matpr.2022.11.235.

Karafillis, A.P., & Boyce, M.C. (1996). Tooling and binder design for sheet metal forming processes compensating spring-back error. *International Journal of Machine Tools and Manufacture*, *36*(4), 503-526. https://doi.org/10.1016/0890-6955(95)00023-2.

Lee, S.Y., Yoon, S.Y., Kim, J.H., Barlat, F., & Oh, K.S. (2023). Evaluation of loading-path-dependent constitutive models for spring-back prediction in martensitic steel forming. *International Journal of Mechanical Sciences*, *251*, 108317. https://doi.org/10.1016/j.ijmecsci.2023.108317.

Ma, J., & Welo, T. (2021). Analytical spring-back assessment in flexible stretch bending of complex shapes. *International Journal of Machine Tools and Manufacture*, *160*, 103653. https://doi.org/10.1016/j.ijmachtools.2020.103653.

Meng, Q., Zhai, R., Zhang, Y., Fu, P., & Zhao, J. (2022). Analysis of spring-back for multiple bending considering nonlinear unloading-reloading behavior, stress inheritance and Bauschinger effect. *Journal of Materials Processing Technology*, *307*, 117657. https://doi.org/10.1016/j.jmatprotec.2022.117657.

Pangaribawa, M.R., Wiyono, S., Sarjito, Sutopo, N.A., & Khusaini, F.A. (2022). Numerically detection fluid characteristic effects in porous media for plastic manufacturing process reconstruction. *International Journal of Mathematical, Engineering and Management Sciences*, *7*(5), 749-763.

Riyadi, T.W.B., Setiadhi, D., Anggono, A.D., Siswanto, W.A., & Al-Kayiem, H.H. (2021). Analysis of mechanical and thermal stresses due to TiN coating of Fe substrate by physical vapor deposition. *Forces in Mechanics*, *4*, 100042. https://doi.org/10.1016/j.finmec.2021.100042.

Shen, H., Li, S., Ni, X., & Chen, G. (2013). A modified displacement adjustment method to compensate for surface deflections in the automobile exterior panels. *Journal of Materials Processing Technology*, *213*(11), 1943-1953.

Siswanto, W.A., & Omar, B. (2009). Die surface design optimization accommodating spring-back assisted by an automatic surface generator. *International Journal of Material Forming*, *2*(1 supplement), 797-800. https://doi.org/10.1007/s12289-009-0500-2.

Suckow, T., Schroeder, J., & Groche, P. (2021). Roll forming of a high strength AA7075 aluminum tube. *Production Engineering*, *15*(3-4), 573-586. https://doi.org/10.1007/s11740-021-01046-2.

Sun, Y., Zhang, Y., Chen, Z., Lin, X., Zhao, X., Li, Y., Yao, S., Wang, X., & Zheng, X. (2022). Investigation on compression-spring-back performance of the SUS301 stainless steel gasket considering the residual stress. *Materials Today Communications*, *33*, 104296. https://doi.org/10.1016/j.mtcomm.2022.104296.

Wagoner, R.H., Lim, H., & Lee, M.G. (2013). Advanced issues in spring-back. *International Journal of Plasticity*, *45*, 3-20. https://doi.org/10.1016/j.ijplas.2012.08.006.

Wei, H., Zhou, L., Heidarshenas, B., Ashraf, I.K., & Han, C. (2019). Investigation on the influence of spring-back on precision of symmetric-cone-like parts in sheet metal incremental forming process. *International Journal of Lightweight Materials and Manufacture*, *2*(2), 140-145. https://doi.org/10.1016/j.ijlmm.2019.05.002.

Xu, Z., Qiu, D., Shahzamanian, M.M., Zhou, Z., Mei, D., & Peng, L. (2023). An improved spring-back model considering the transverse stress in microforming. *International Journal of Mechanical Sciences*, *241*, 107947. https://doi.org/10.1016/j.ijmecsci.2022.107947.

Yaguang, L., Zhenye, L., Zhiheng, Z., Tianxia, Z., Dayong, L., Shichao, D., Hua, X., & Lei, S. (2019). An analytical model for rapid prediction and compensation of spring-back for chain-die forming of an AHSS U-channel. *International Journal of Mechanical Sciences*, *159*, 195-212. https://doi.org/10.1016/j.ijmecsci.2019.05.046.

Zhang, Q.F., Cai, Z.Y., Zhang, Y., & Li, M.Z. (2013). Spring-back compensation method for doubly curved plate in multi-point forming. *Materials and Design*, *47*, 377-385. https://doi.org/10.1016/j.matdes.2012.12.005.

Zhang, Z., Wu, J., Zhang, S., Wang, M., Guo, R., & Guo, S. (2016). A new iterative method for spring-back control based on theory analysis and displacement adjustment. *International Journal of Mechanical Sciences*, *105*, 330-339. https://doi.org/10.1016/j.ijmecsci.2015.11.005.

Zhu, Y.X., Liu, Y.L., Yang, H., & Li, H.P. (2013). Improvement of the accuracy and the computational efficiency of the spring-back prediction model for the rotary-draw bending of rectangular H96 tube. *International Journal of Mechanical Sciences*, *66*, 224-232. https://doi.org/10.1016/j.ijmecsci.2012.11.012.